# Chapter 18
# NICMOS Data Analysis

**In This Chapter...**



This chapter describes specific tools and topics related to the analysis of the NICMOS data. The first section points out some STSDAS tools for analyzing NICMOS images. The remainder of the chapter deals with topics of more or less general interest: photometric calibration, PSF subtraction, and polarimetric analysis.

## 18.1 STSDAS Software

Software tools for NICMOS FITS files now available in the STSDAS packages **toolbox.imgtools.mstools** and **hst_calib.nicmos** have been designed to maintain compatibility with pre-existing analysis software. The tools have either been written in ANSI-C or are IRAF CL scripts interfacing with pre-existing IRAF/STSDAS tasks. Some of the new tools will accept a variety of data formats such as OIF and GEIS, as well as STIS and NICMOS FITS files, and will in time replace the STSDAS tasks they render obsolete.

The new tasks fall into two major categories:

1. ***General-purpose utilities***. These tasks include tools for mathematical and statistical operations on science images and for analysis and display of reduced and raw data. In most cases, the new utilities extend existing routines to include error and data quality propagation. These are the utilities of greatest interest to the user community. Under this category are several

tasks described in Chapter 3, **msarith**, **mscombine**, **msstatistics**, **msjoin** and **mssplit**, along with a few other tasks we describe below, **ndisplay**, **markdq**, and **pstack**. The first five are found in the package **toolbox.imgtools.mstools**, the remaining ones reside in the package **hst_calib.nicmos**.

2. ***Calibration-oriented utilities***. These tasks generate reference files, such as readnoise arrays, dark files, flatfields, non-linearity correction arrays, and bad pixel arrays, to feed the calibration database and to support the calibration pipelines. The tasks are designed specifically for the calibration of NICMOS and will not be of general utility. The tools are **mstreakflat**, **msbadpix**, **ndark**, **nlincorr**, and **msreadnoise**. All are located in the calibration package **hst_calib.nicmos**.

The tasks in the **toolbox.imgtools.mstools** package are particularly useful for working with individual STIS and NICMOS imsets. See “Working with STIS and NICMOS Imsets” on page 3-12 if you are not familiar with these tasks. Below we describe a few tasks of specific interest to NICMOS observers. For additional details and examples of these and other tools, please refer to the online help.



### ndisplay and markdq

The **markdq** task reads the data quality (DQ) array from a NICMOS image and marks the DQ flags on the displayed image. Each flag value can be set independently to a different color or can be turned off. The **ndisplay** task combines the capabilities of the IRAF task **display** and the task **markdq**: it displays a NICMOS image and overlays the DQ flags according to a user-specified color-code. Both tasks are useful for locating specific DQ values, for example, the cosmic rays rejected by **calnica** in a MULTIACCUM image.

### pstack

The **pstack** task plots all the samples of the specified pixels from a NICMOS MULTIACCUM image as a function of time. This task can be used to track the time behavior of an image on a pixel-by-pixel basis. For example, the temporal positions of cosmic ray hits or the onset of saturation during the course of an exposure can be located for a defined set of pixels.

## 18.2 Photometric Calibrations

Being above the atmosphere, NICMOS is not forced to adopt filter bandpasses like instruments used at ground-based observatories, but instead it has filters constrained by anticipated scientific demands. Thus in practice NICMOS does not have filters matched to any of the ground-based photometric bands. Obtaining photometric calibrations for NICMOS data is discussed in this section; cases of continuum sources, emission lines, and grism spectra will be presented.

### 18.2.1 Units for NICMOS Photometry

Given the multitude of units and systems that have been used for infrared (IR) photometry (magnitudes, Jy, W $m^{-2}$ $\mu m^{-1}$, erg $sec^{-1}$ $cm^{-2}$ $\mu m^{-1}$, etc.) and given the lack of a standard for ground-based IR filters, NICMOS has adopted the IRAS approach, where the calibrated data were presented in Janskys (Jy), or Jy $arcsec^{-2}$ for surface brightness data. Details on how to transform different sets of units can be found in Chapter 12 of the *NICMOS Instrument Handbook* or obtained using the Unit Conversion Program in the NICMOS WWW software tools page.

### 18.2.2 Fluxes and Magnitude Zeropoints

The NICMOS calibration pipeline provides two photometric parameters for the conversion of countrates into fluxes. These parameters are found in the keywords PHOTFNU and PHOTFLAM in the header of the calibrated image. PHOTFNU is given in units of Jy sec $DN^{-1}$ and PHOTFLAM in units of ergs $cm^{-2}$ $Å^{-1}$ $DN^{-1}$. Because NICMOS calibrated data are given in countrate, i.e., DN $sec^{-1}$, the countrate to flux conversion is simply achieved by multiplying the countrate by the PHOTFNU or PHOTFLAM value, depending on which units are desired for the final calibrated image.

A list of current PHOTFNU and PHOTFLAM values for all available filters are given in Table 18.1 through Table 18.3. These values are the result of the on-orbit SMOV photometric characterization and are preliminary. The SMOV photometric characterization used a small subset of filters for each of the cameras; a full calibration of NICMOS photometric performance as a function of wavelength is not available yet. Our best estimates indicate that the values listed in the tables have uncertainties at the 10–15% level, on average. A complete characterization of NICMOS photometric performance will be obtained as part of the Cycle 7 calibration program and the PHOTFNU and PHOTFLAM values will then be updated. The revised photometric table will then be posted on the NICMOS WWW pages.

In the header of your calibrated images, there are three additional photometric parameters that characterize the filter used for the observation (PHOTPLAM and PHOTBW) and provide the ST magnitude zero point (PHOTZPT). PHOTPLAM gives the value of the pivot wavelength of the filter in Angstroms. This wavelength is source-independent and is the wavelength for which:

$$PHOTFLAM = c \times PHOTFNU \times PHOTPLAM^{-2}$$

where *c* is the speed of light in vacuum. PHOTBW gives the rms band of the filter in Angstroms (see the *Synphot User's Guide* for a detailed definition of both parameters).

The magnitude of an object can be determined in the ST system (e.g., based on a constant flux per unit wavelength) using the photometric zero-point keyword PHOTZPT (= -21.1) simply by:

$$m_{ST} = -2.5\log(PHOTFLAM \times CR) + PHOTZPT$$

$$= -2.5\log(PHOTFLAM \times CR) - 21.1$$

where *CR* is the count rate in units of DN $sec^{-1}$. On the other hand, the magnitude in Oke's $AB_\nu$ system (e.g., based on a constant flux per unit frequency) is obtained by applying the following expression:

$$m_{AB} = -2.5\log(10^{-23} \times PHOTFNU \times CR) - 48.6$$

$$= -2.5\log(PHOTFNU \times CR) + 8.9$$



Zeropoints for magnitudes based on the Vega system are reported in the last column of Table 18.1 through Table 18.3 in units of Jy. The zeropoints for the NICMOS bandpasses are derived from the reference spectrum of Vega generated at the STScI (Colina, Bohlin & Castelli 1996, ISR CAL/SCS-008), assuming Vega has a magnitude equal to 0.02 in all NICMOS bandpasses, as per the calibration of Campins et al. (1985, *AJ*, 90, 896). The reference spectrum has been multiplied by a factor 1.05 to correct for the 5% discrepancy between the model and the near infrared measurements. The conversion from count rates to magnitudes in the Vega system is given by the standard formula:

$$m = -2.5\log(PHOTFNU \times CR \times ZP(Vega)^{-1})$$

Details about plans to define an HST JHK system and compute the photometric transformations to ground-based systems are given in "Magnitudes and Photometric Systems Transformations" on page 18-8.

## 18.2.3 Photometric Corrections

### Differential Photometry

The photometric values provided in the headers are obtained from measurements of standard stars in the central regions of the detectors. Both high frequency (pixel-to-pixel) and low frequency (large-scale structures) sensitivity variations will be corrected using on-orbit flats. Preliminary SMOV differential photometry characterization of NICMOS cameras indicate that residual large scale deviations could amount to ~2%, except in the corners that might be higher. A Cycle 7 calibration program has been designed to measure with a fine grid the photometric deviations from the average as a function of wavelength, for each camera. A correction image might be generated as a product of this program, if measurable deviations are found.

**Table 18.1:** NIC1 Photometry

| Spectral Element | PHOTFLAM (erg $cm^{-2}$ $A^{-1}$ $DN^{-1}$) | PHOTNU (Jy sec $DN^{-1}$) | ZP(Vega) (Jy) |
|---|---|---|---|
| F090M | 5.349E-18 | 1.459E-5 | 2305.9 |
| F095N | 7.634E-17 | 2.316E-4 | 1854.1 |
| F097N | 6.163E-17 | 1.941E-4 | 2372.0 |
| F108N | 3.614E-17 | 1.411E-4 | 2011.8 |
| F110M | 1.739E-18 | 7.051E-6 | 1947.2 |
| F110W | 6.379E-19 | 2.713E-6 | 1897.0 |
| F113N | 2.922E-17 | 1.244E-4 | 1890.9 |
| F140W | 2.253E-19 | 1.558E-6 | 1395.4 |
| F145M | 9.020E-19 | 6.376E-6 | 1278.9 |
| F160W | 3.266E-19 | 2.814E-6 | 1111.6 |
| F164N | 7.323E-18 | 6.618E-5 | 1018 |
| F165M | 6.120E-19 | 5.551E-6 | 1032.5 |
| F166N | 6.975E-18 | 6.416E-5 | 1080.1 |
| F170M | 5.306E-19 | 5.156E-6 | 1011.1 |
| F187N | 5.051E-18 | 5.922E-5 | 826.6 |
| F190N | 4.842E-18 | 5.822E-5 | 861.5 |
| POL0S | 1.171E-18 | 4.392E-6 | 2027.9 |
| POL120S | 1.171E-18 | 4.392E-6 | 2027.9 |
| POL240S | 1.171E-18 | 4.392E-6 | 2027.9 |



## Pixel Centering

As with many other array detectors, the sensitivity of the NICMOS detectors is lower near the edges of the pixels than in their centers. It is as though there were small regions of reduced sensitivity along the intra-pixel boundaries. In practical terms this effect means that for a source whose flux changes rapidly on a size comparable with or smaller than the pixel size, the measured countrate, and therefore flux, will depend on where the center of the source lies with respect to the center of the pixel. Because this position is not known a priori, this effect will introduce some uncertainty in the flux calibration for a point source. This uncertainty will be largest (no more than a few percent, we expect) for NIC3 at short wavelengths, in which the PSF is undersampled. For high precision photometry and to compute the amount of photometric uncertainty in a particular camera and filter combination due to this effect, subpixel dithering is recommended.

**Table 18.2:** NIC2 Photometry

| Spectral Element | PHOTFLAM (erg cm-2 A-1 DN-1) | PHOTNU (Jy sec $DN^{-1}$) | ZP(Vega) (Jy) |
|---|---|---|---|
| F110W | 5.626E-19 | 2.390E-6 | 1898.3 |
| F160W | 2.939E-19 | 2.529E-6 | 1113.0 |
| F165M | 5.484E-19 | 4.990E-6 | 1051.1 |
| F171M | 1.232E-18 | 1.217E-5 | 995.4 |
| F180M | 1.185E-18 | 1.277E-5 | 931.5 |
| F187N | 4.336E-18 | 5.079E-5 | 828.2 |
| F187W | 3.858E-19 | 4.509E-6 | 873.1 |
| F190N | 4.293E-18 | 5.171E-5 | 860.6 |
| F204M | 5.946E-19 | 8.217E-6 | 766.0 |
| F205W | 9.167E-20 | 1.312E-6 | 752.5 |
| F207M | 3.787E-19 | 5.478E-6 | 734.6 |
| F212N | 2.325E-18 | 3.490E-5 | 710.9 |
| F215N | 2.493E-18 | 3.840E-5 | 690.0 |
| F216N | 2.236E-18 | 3.494E-5 | 648.1 |
| F222M | 3.099E-19 | 5.086E-6 | 652.9 |
| F237M | 2.329E-19 | 4.363E-6 | 584.0 |
| POL0L | 3.164E-19 | 4.225E-6 | 785.1 |
| POL120L | 3.164E-19 | 4.225E-6 | 785.1 |
| POL240L | 3.164E-19 | 4.225E-6 | 785.1 |



## PSF Variations

The point spread function (PSF) of the telescope changes with time, and these changes will affect photometry using very small (less than 3-4 pixel radius) apertures. Changes in focus observed on an orbital timescale are due mainly to thermal breathing of the telescope. In addition to this short term PSF variation there is an additional long-term NICMOS component, as the cryogen evaporates and the dewar relaxes. As a result of the stress produced by the solid nitrogen on the instrument, NICMOS detectors have been moving, and keep moving, along the focus direction. The motion of the cameras is monitored twice a month and NICMOS focus updates can be periodically implemented, if required. Although preliminary results from SMOV indicate that the breathing effects on small aperture photometry are below our measurement precision (a few percent), the subject is still under investigation.

**Table 18.3:** NIC3 Photometry

| Spectral Element | PHOTFLAM (erg cm-2 A-1 DN-1) | PHOTNU (Jy sec $DN^{-1}$) | ZP(Vega) (Jy) |
|---|---|---|---|
| F108N | 4.335E-17 | 1.687E-4 | 2021.2 |
| F110W | 6.794E-19 | 2.875E-6 | 1903.9 |
| F113N | 3.315E-17 | 1.408E-4 | 1894.8 |
| F150W | 2.008E-19 | 1.606E-6 | 1238.2 |
| F160W | 3.462E-19 | 2.985E-6 | 1111.1 |
| F164N | 7.738E-18 | 6.993E-5 | 1032.5 |
| F166N | 7.778E-18 | 7.135E-5 | 1081.5 |
| F175W | 9.150E-20 | 1.029E-6 | 971.5 |
| F187N | 5.220E-18 | 6.120E-5 | 826.6 |
| F190N | 4.994E-18 | 6.015E-5 | 860.6 |
| F196N | 4.227E-18 | 5.438E-5 | 809.9 |
| F200N | 3.810E-18 | 5.070E-5 | 791.1 |
| F212N | 2.675E-18 | 4.016E-5 | 710.9 |
| F215N | 2.854E-18 | 4.396E-5 | 689.9 |
| F222M | 3.519E-19 | 5.777E-6 | 652.8 |
| F240M | 2.017E-19 | 3.865E-6 | 571.7 |
| G096 | 1.641E-18 | 5.560E-6 | 2138.9 |
| G141 | 2.614E-19 | 2.102E-6 | 1235.5 |
| G206 | 8.583E-20 | 1.178E-6 | 817.9 |



## Aperture Correction

It is often difficult to measure the total flux of a point source due to the extended wings of the PSF, difraction spikes, and scattered light. Such measurements are particularly difficult in crowded fields where the extended wings of well resolved sources can overlap with each other. An accurate method of measuring the integrated flux in these situations could consist of several steps:

1. Measure in the image the total counts within a small radius.
2. Simulate the TinyTim[1] PSF for the particular camera-filter combination and position in the detector.
3. Measure in the simulated PSF image the fraction of total flux within the selected aperture.

1. TinyTim software can be retrieved from the Web at:
`http://scivax.stsci.edu/~krist/tinytim.html`

To obtain the total flux of the source, the countrate then only needs to be multiplied by the PHOTFNU or PHOTFLAM value and by the inverse of the measured fraction obtained in step three above.

Empirical PSFs could also be used for the above mentioned method. However, there are no plans to obtain PSF profiles for all camera and filter combinations as part of the Cycle 7 calibration plan. Empirical PSFs for the central regions of the detectors can be obtained from the calibrated images obtained for the Cycle 7 absolute photometry (proposal 7691) and photometric monitoring (proposal 7607) programs.

### Red Leaks

Many very red targets will be observed with NICMOS at short wavelengths (~1 μm). For these sources the flux at ~2.2–2.5 μm could be orders of magnitude larger than at ~1.0 μm and therefore exceptionally good out-of-band blocking would be required. Pre-launch tests indicated that for very red sources (temperature ~700 K and lower), the photometric errors induced by red leaks might be as large as an order of magnitude in a few filters. The filters for which red leaks might be a problem are: F090M, F095N, F097N, F108N, F110M, F110W, F113N, F187N and F190N. Strategies involving observations in multiple filters to model the source spectral energy distribution are required in these cases. Observations of a very red star will be obtained as part of the Cycle 7 calibration plan and the results will be posted on the Web.

### Non-Zero Zeroth Read Correction for Bright Sources

The problem of the non-zero zeroth read for bright sources was discussed in Chapter 17. If a non-zero zeroth read is present, corrections for the detector's non linear response may not have been taken into proper account by the current version of the pipeline (as of August 1997). It is advisable to reprocess the data with the most recent version of the calibration software (at the time of this writing, early August 1997, the software modification for **calnica** that should remove the problem in the pipeline is under testing; data processed after the new software is installed in the pipeline should be free of the non-zero zero read problem).

## 18.2.4 Magnitudes and Photometric Systems Transformations

As previously mentioned, NICMOS data will be calibrated in units of Jy or Jy arcsec$^{-2}$. There are currently no plans to compute color corrections and to provide transformations to convert HST fluxes into ground-based magnitude systems. However, as part of the Cycle 7 absolute photometry program, we will observe a few blue stars (white dwarfs), intermediate color stars (solar analogs), and very red stars covering a large range in color (Table 18.4). The calibrated data will be made available immediately for users requiring to transform their HST fluxes into any ground-based system. The recommended HST JHK-analog system is obtained using the F110W, F160W and F222M filters.

**Table 18.4:** List of Stars for Photometric Transformations

| Name | H | J-H | H-K | Status |
|---|---|---|---|---|
| G191-B2B | 12.6 | -0.10 | -0.14 | Primary standard (white dwarf). |
| P330E | 11.6 | 0.28 | 0.07 | Primary standard (solar analog). |
| OPH-S1 | 7.3 | 1.53 | 0.94 | Primary standard (red standard). |
| GD71 | 13.8 | -0.08 | -0.13 | Pending approval (white dwarf). |
| P177D | 12.0 | 0.28 | 0.06 | Pending approval (solar analog). |
| CSKE_12 | 9.5 | 2.08 | 0.89 | Pending approval (red standard). |
| BRI0021 | 11.1 | 0.75 | 0.52 | Pending approval (red standard). |

## 18.2.5 Absolute Photometry for Emission Line Filters

The narrow band filters in NICMOS are intended primarily for observations of emission or absorption lines in sources. Because the photometric conversion factors PHOTFNU and PHOTFLAM for all NICMOS filters are obtained from continuum observations of emission-line free standard stars, the flux in erg $sec^{-1}$ $cm^{-2}$ of an emission line is given by the expression:

$$Flux_{line} = 1.054 \times FWHM \times PHOTFLAM \times CR$$

where FWHM is the full width half maximum of the equivalent gaussian filter to the narrow-band filter used (see Chapter 11 of the *NICMOS Instrument Handbook*), and we have assumed that the continuum has been already subtracted from the total flux in the filter and that the line is centered in the filter. If the emission line is not at the central wavelength of the filter, the line flux will need correction for the filter transmission curve. To estimate the variation in the absolute flux due to the positioning and width of the emission line in the filter bandpass, the **synphot** task **calcphot** can be used as shown below. See the *Synphot User's Guide* for additional help.

**Figure 18.1:** Estimating Absolute Flux Variation

```
sy> epar calcphot
obsmode = nicmos,3,f212n,dn Instrument observation mode
spectrum= gauss(21200,40)*unit(1E-13,flam) Synthetic spectrum to calculate
form = counts Form for output data
(func = effstim) Function of output data
(vzero = ) List of values for variable zero
(output = none) Output table name
(append = no) Append to existing table?
(wavetab= ) Wavelength table name
(result = 0.) Result of synphot calculation for form
(refdata= ) Reference data
(mode = a)

sy> epar calcphot
obsmode = nicmos,3,f212n,dn Instrument observation mode
spectrum= gauss(21280,40)*unit(1E-13,flam) Synthetic spectrum to calculate
form = counts Form for output data
(func = effstim) Function of output data
(vzero = ) List of values for variable zero
(output = none) Output table name
(append = no) Append to existing table?
(wavetab= ) Wavelength table name
(result = 0.) Result of synphot calculation for form
(refdata= ) Reference data
(mode = a)
```



The examples above compute the countrate in the NIC3 F212N filter for a $H_2$ (2.12 micron) emission line having a gaussian profile of 40 Angstroms and a peak flux of 1.0 x $10^{-13}$ erg $sec^{-1}$ $cm^{-2}$ $A^{-1}$. The integrated flux will then be 4.2 x $10^{-12}$ erg $sec^{-1}$ $cm^{-2}$. In the first example the $H_2$ emission line is at zero redshift and centered on the filter while in the second example the line is redshifted by 80 Angstroms. If the emission line is centered on the filter, the $H_2$ flux will produce 7421.1 DN $sec^{-1}$ while the countrate will be ~90% of this value (i.e., 6662.3 DN $sec^{-1}$) for the redshifted emission line. The expression for the $Flux_{line}$ above can be directly applied to the first case, while a correction factor 1.11=(7421.1/6662.2) is needed in the second case.

## 18.2.6 Absolute Spectrophotometry with NICMOS Grisms

The accuracy of the absolute spectrophotometry with NICMOS grisms depends on three different limiting factors:

- Accuracy of the spectral energy distribution of the standard stars used to obtain the inverse sensitivity curve.
- Quality of the flat-fielding and background subtraction of the calibration observations.
- Quality of the flat-fielding and background subtraction of the science observation itself.

The major source of uncertainty in the absolute spectrophotometry of a given source comes from the variability and structure of the background. Every pixel on the NIC3 array will receive background radiation over the entire spectral bandpass of the particular grism, while the source spectrum will be dispersed. The accuracy of the background subtraction is limited by our knowledge of the spectral response of each pixel, which is somewhat different from pixel to pixel. Extracted

spectra will have to be corrected for the spectral response of each pixel. The accuracy of this correction is again limited by our knowledge of the detector response.

The absolute flux calibration of the spectral energy distribution of the standard stars in the 0.8 to 2.5 μm wavelength range is known to 2–5%. Characterization of the grisms' absolute sensitivity during SMOV indicates that the absolute calibration of grism spectrophotometry for bright sources, i.e. well above background, will have a total 20–30% uncertainty. For Grism C the uncertainties could be even higher because of the large thermal background in this wavelength range (1.4 to 2.5 μm).

## 18.3 PSF Subtraction

Accurate PSF subtraction is a prime concern for an observer wishing to study faint features around bright objects. Typical situations are: host galaxy harboring a bright quasar; circumstellar nebulosity around a bright star; faint companions of a bright star, etc. The PSF subtraction technique has proved to be very successful in this kind of studies for HST data obtained with WFPC2. But imaging with NICMOS cameras 1 and 2 can probably easily exceed the success of WFPC2 thanks to a few important advantages:

- Cameras 1 and 2 provide images which are diffraction limited, well sampled, and better resolved (see Figure 18.1 and Figure 18.2).
- The MULTIACCUM mode automatically provides sub-exposures at different times as a way to look at increasingly faint features at different distances from the bright central source.
- For saturated bright central point source, there is no blooming along the detector array columns.

The best way to get a high quality PSF for PSF subtraction is to measure an isolated bright unsaturated star in the same image or to construct a composite PSF using good stars in the image. This can be accomplished using the IRAF **digiphot** package as described in *A User's Guide to Stellar CCD photometry with IRAF*[2]. A PSF obtained from the same image, along with a number of obvious advantages, also takes care of the *breathing* effect (variations of focus position due to thermally induced mechanical displacements in the HST optical path). If no suitable star can be found in the image, one can resort to a synthetic PSF computed using TinyTim.



2. This and other relevant IRAF documents can be obtained from the IRAF Web site at: `http://iraf.noao.edu/`.

**Figure 18.2:** NIC1 Image with PSF Radial Profile

**Image of Star Taken with NIC1 F165M** **PSF Radial Profile**

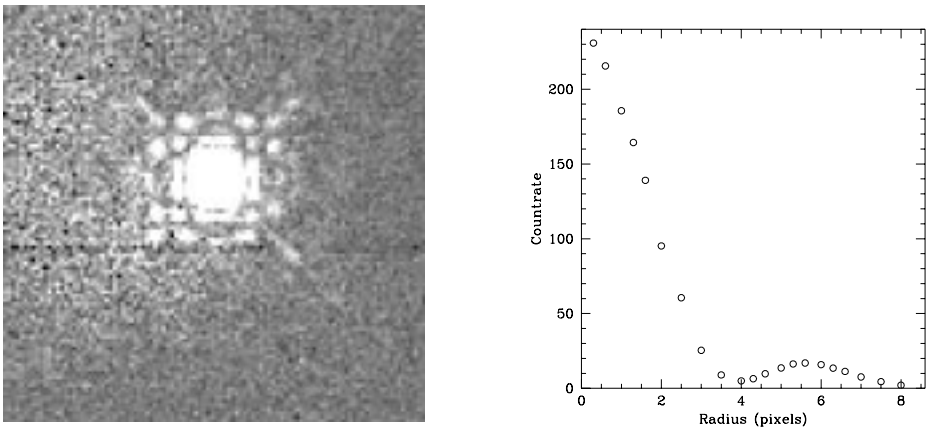


**Figure 18.3:** NIC2 Image with Radial Profile

**Image of Star Taken with NIC2 F237M** **PSF Radial Profile**

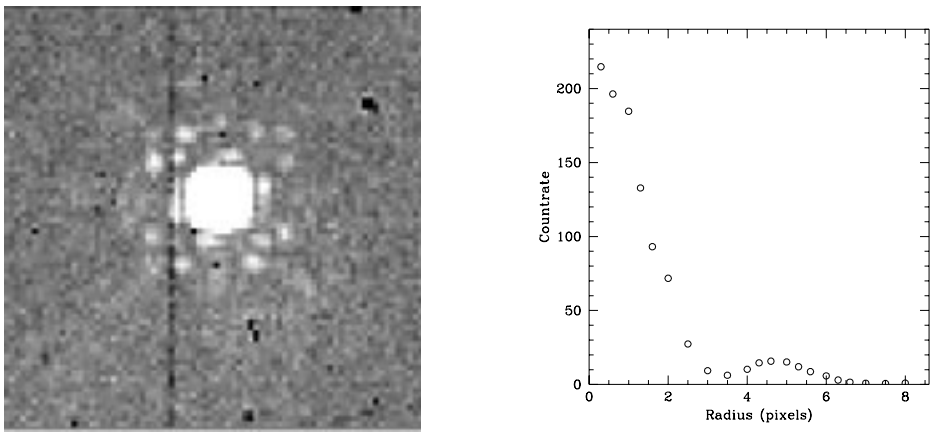




# 18.4 Analysis of Polarization Images

## 18.4.1 Introduction

The analysis of NICMOS polarization images is aimed at determining the Stokes' Parameters, and from those the polarization angle and degree for each pixel. NICMOS Camera 1 and Camera 2 each contain three polarizers, whose principal axes of transmission are separated by 120 degrees. The spectral coverage is fixed for each Camera, with wavelength coverage 0.8–1.3 μm in Camera 1 and 1.9–2.1 μm in Camera 2. A complete set of polarimetric observations will contain images obtained in all three polarizers of the selected wavelength range. We assume that each image has been processed through **calnica** and **calnicb** to produce a fully reduced and (if necessary) mosaiced image in each of the three

filters, with the data corrected for saturation and cosmic rays and converted to flux density.

The images in the three filters need to be compared, in order to produce the Stokes' parameters. To do so, the three images need to have the same dimensions and to be registered (have the source centered at exactly the same location in each image). In principle they should already be registered, provided the images in each filter were taken in the same visit without any changes of guide stars. If there is any displacement of the source between images, then each image can be registered using the IRAF task **imlintran**. When **imlintran** is used, the origin for the three input images should be set to the location of the source in each, so that in the output images the origin and the parameters *nlines* and *ncolumns* are identical.

To generate Stokes' parameters, the relative differences in flux between images in the different polarizing filters are used. Where the signal level is very faint, and the signal-to-noise ratio is very low, the differences will be very large but dominated by noise. If you attempt to calculate the Stokes' parameters using such data, you will obtain large and entirely spurious polarizations. To avoid this problem, it is advisable to estimate the noise in an area of the image free of sources, and then set a threshold at a value of order five to ten times this noise level. Using the IRAF task **imreplace**, all pixels with signals below this threshold should be set to some arbitrary value, probably close to the measured noise level. This action will cause all areas of the image where the signal level is very faint to show zero polarization.



## 18.4.2 Theory

If we define the intensity and statistical uncertainties (including read-noise) obtained in the three polarizers to be $I_0$, $I_{120}$ and $I_{240}$ and $\sigma_0$, $\sigma_{120}$, $\sigma_{240}$ respectively, then we may obtain the total intensity *I* from:

$$I = \frac{2}{3}(I_0 + I_{120} + I_{240})$$

and the Stokes parameters Q and U:

$$Q = \frac{2}{3}(2I_0 - I_{240} - I_{120})$$

$$U = \frac{2}{\sqrt{3}}(I_{240} - I_{120})$$

The statistical uncertainties are obtained by straightforward propagation of errors:

$$\sigma_I = \frac{2}{3}\sqrt{[\sigma_0^2 + \sigma_{240}^2 + \sigma_{120}^2]}$$

$$\sigma_U = \frac{2}{\sqrt{3}}\sqrt{[\sigma_{240}^2 + \sigma_{120}^2]}$$

$$\sigma_Q = \frac{2}{3}\sqrt{[4\sigma_0^2 + \sigma_{240}^2 + \sigma_{120}^2]}$$

The Stokes parameters can then be combined to yield the polarized intensity, $I_{p:}$

$$I_p = [Q^2 + U^2]^{1/2}$$

and the degree, *P*, and position angle of polarization, *q*, using:

$$P = \frac{I_P}{I}$$

$$\theta = 28.648 \tan^{-1}\left(\frac{U}{Q}\right)$$



## 18.4.3 A Useful Script for Polarization Analysis

At the time of writing, we do not yet have NICMOS versions of all the IRAF software tools needed to solve these equations for our polarization images.

An interactive procedure to derive relevant parameters from NICMOS polarization images has been developed by Hines et al. (1997).[3] In addition to taking into account instrumental polarization, this routine corrects for flatfield uncertainties and for small shifts between the images.

However, first approximation results can be obtained with a straightforward IRAF script. The approach we follow here is the simplest possible path to determining the polarization properties from the data. It does not take into account the instrumental polarization and does not allow for systematic errors in the data. The script will yield the correct morphology but not the exact intensity of the polarization. There are more sophisticated tools available in the community, including the one referenced above, which have been developed specifically to analyze polarization images, and which will yield better results than this very simple approach. The IRAF script is included below, and is commented.

3. Hines, D.C., G.D. Schmidt, and D. Lytle, 1997, "The Polarimetric Capabilities of NICMOS," *HST Calibration Workshop*, S. Casertano et al. (eds.)

The script doesn't take into account that in NIC1 the POL120 filter has only 48% transmission, while the POL0 filter has 98% transmission. For sake of simplicity, we assume here that the polarization image at 120 degrees has been obtained using the POL0 filter with a spacecraft roll, rather than using the POL120 filter.

**Figure 18.4:** Polarization Script

```
procedure pol( )
begin
!use `flpr' to flush the process cache regularly to prevent IRAF !memory problems

!first generate the total intensity, pols_i
msarith("pol0s","+","pol120s","tmp1")
msarith("tmp1","+","pol240s","tmp2")
msarith("tmp2","*", 0.6666667,"pols_i")
imdel("tmp1")
imdel("tmp2")
flpr

!now generate Stokes Q parameter, pols_q...
msarith("pol0s","*", 2.0, "tmp1")
msarith("tmp1", "-","pol240s","tmp2")
msarith("tmp2", "-","pol120s","tmp3")
msarith("tmp3", "*", 0.6666667," pols_q")
flpr
imdel("tmp1")
imdel("tmp2")
imdel("tmp3")
flpr

!...and next the Stokes' U parameter, pols_u...
msarith("pol240s","-","pol120s", "tmp1")
msarith("tmp1", "*", 1.154701, "pols_u")
imdel("tmp1")
flpr

!...now the polarized intensity...
msarith ("pols_q","*","pols_q","tmp1")
msarith ("pols_u","*","pols_u","tmp2")
msarith ("tmp1", "+","tmp2", "tmp3")
flpr

!...this messy bit is to generate the uncertainty on the polarized !intensity...
imfunction("tmp3", "tmp4.fits","sqrt")
imarith ("tmp3[2]", "*", 0.5, "tmp5.fits")
!cp tmp3.fits pols_ip.fits
imcopy ("tmp4","pols_ip[1][1:256,1:256]")
imcopy ("tmp5","pols_ip[2][1:256,1:256]")
flpr
imdel("tmp1") imdel("tmp2") imdel("tmp3") imdel("tmp4") imdel("tmp5")
flpr

!...now here is the degree of polarization, pols_p...
msarith("pols_ip","/","pols_i","pols_p")

!...and finally, here comes the polarization angle, pols_theta...
msarith("pols_u","/","pols_q","tmp1")
flpr
imfunction("tmp1","tmp2.fits","atan")
!cp tmp1.fits pols_theta.fits
imarith ("tmp2", "*", 28.648, "tmp3.fits")
flpr
imcopy ("tmp3","pols_theta[1][1:256,1:256]")
imarith ("tmp1[2]", "/", "tmp1[1]", "tmp4.fits")
imarith ("pols_theta[1]", "*", "tmp4", "tmp5.fits")
flpr
imcopy ("tmp5", "pols_theta[2][1:256,1:256]")
imdel("tmp1")
imdel("tmp2")
imdel("tmp3")
imdel("tmp4")
imdel("tmp5")
flpr
end
```

The script assumes we started with three images, named `pol0s.fits`, `pol120s.fits` and `pol240s.fits`, taken in the short wavelength polarization filters. The output from the script is a set of files named `pols_u.fits` and `pols_q.fits` (the Stokes' U and Q parameters respectively), `pols_i.fits` (the total intensity), `pols_ip.fits` (the polarized intensity), `pols_p.fits` (the degree of polarization), and `pols_theta.fits` (the polarization angle). The error propagation should, in general, be more or less correct for statistical errors (all systematic errors are ignored), although for the polarization angle the error is a gross approximation. When a new version of the IRAF **imfunction** task is written to include error propagation, the rather messy parts of the above script which generate error arrays will no longer be needed.